Controllable optical rogue waves in the femtosecond regime

Chao-Qing Dai (戴朝卿),[1,2] Guo-Quan Zhou (周国泉),[1] and Jie-Fang Zhang (张解放)[2,3]
[1]*School of Sciences, Zhejiang Agriculture and Forestry University, Lin'an, Zhejiang CN-311300, China*
[2]*School of Physical Science and Technology, Suzhou University, Suzhou, Jiangsu CN-215006, China*
[3]*Zhejiang University of Media and Communications, Hangzhou CN-310018, China*
(Received 21 July 2011; revised manuscript received 13 October 2011; published 13 January 2012)

We derive analytical rogue wave solutions of variable-coefficient higher-order nonlinear Schrödinger equations describing the femtosecond pulse propagation via a transformation connected with the constant-coefficient Hirota equation. Then we discuss the propagation behaviors of controllable rogue waves, including recurrence, annihilation, and sustainment in a periodic distributed fiber system and an exponential dispersion decreasing fiber. Finally, we investigate nonlinear tunneling effects for rogue waves.

DOI: 10.1103/PhysRevE.85.016603 PACS number(s): 05.45.Yv, 42.65.Tg

I. INTRODUCTION

Rogue waves (or freak waves), single ocean waves with amplitudes significantly larger (two, three, or more times higher) than the surrounding average wave crests, were considered mysterious until recorded for the first time by scientific measurements during an encounter at the Draupner oil platform in the North Sea [1]. These rogue waves have been considered myths for a long time. Although they are elusive and intrinsically difficult to monitor due to their fleeting existences, as the theoretical and experimental research continues, rogue waves have been observed in many fields, and massive effort has been devoted to study them [2–6].

Good agreement with an approximate dynamical-statistical theory has been found [2]. A statistical model has been developed that predicts for a given mean sea state the probability of occurrence of extreme events [3]. Peregrine identified the key role of the modulational instability (MI) in the formation of patterns resembling freak waves; in particular, as early as 1983 he attracted attention to algebraic breather (also called Peregrine soliton) solutions of the nonlinear Schrödinger equation (NLSE), which can serve as a weakly nonlinear prototype of a freak-wave [4]. So far two main generic mechanisms have been identified in the absence of wave-current interaction: the Benjamin-Feir (BF) [4,5] or modulational instability [6] and an essentially linear space-time focusing [7].

Interestingly enough, the NLSE not only gives a suitable description of rogue water waves, but it is also the governing equation for light pulse propagation in nonlinear optical fibers and matter waves in Bose-Einstein condensates (BECs). Thus, nonlinear optical fibers and BECs provide a good test bed for the study of rogue waves [8–15]. In nonlinear optics, Solli *et al.* [8] have made considerable progress by observing a randomly created optical rogue wave in a photonic crystal fiber and coined the term "optical rogue waves," based on striking phenomenological and physical similarities between the extreme events of the optical system and oceanic rogue waves. Thus from phenomena, we can consider exceptionally high-amplitude optical pulses as optical rogue waves. Kasparian *et al.* [9] experimentally observed optical rogue wave statistics during high-power femtosecond pulse filamentation in air. Akhmediev's breather theory [10] and MI were also linked experimentally in nonlinear optical fibers [11]. Moreover, Erkintalo *et al.* [12] experimentally studied the characteristics of optical rogue waves in supercontinuum generation in the femtosecond regime. More recently, the optical rogue waves observed initially grow from noise, and it is possible to control both the spectral extent and, most importantly, the noise in the supercontinuum [13]. Discrete rogue waves have also been demonstrated [14]. Until now, only randomly created rogue waves have been observed experimentally [8,9,11–13]. Moreover, Ankiewicz *et al.* [15] also investigated theoretical rogue waves and rational solutions of the Hirota equation. Erkintalo *et al.* [16] experimentally studied the characteristics of optical rogue waves in supercontinuum generation in the femtosecond regime. As analyzed in this paper, these processes involve the restraint, annihilation, postponement, and sustainment of rogue waves.

Historically, the study of soliton tunneling effects governed by the variable-coefficient (vc) NLSE began with the pioneering work of Serkin *et al.* [17] since Newell predicted the tunneling effect that exists in nonlinear media in 1978 [18]. Subsequently, the tunneling effects of solitons governed by various vcNLSE have been extensively discussed. For instance, Yang *et al.* [19] confirmed the compression of the optical pulse by a nonlinear barrier. Wang *et al.* [20] discussed the tunneling effects of spatial similaritons passing through the nonlinear barrier (or well). Dai *et al.* [21] studied the tunneling effects of bright and dark similaritons in the birefringent fiber. Zhong *et al.* [22] presented the nonlinear tunneling effects of spatial solitons in the nonlinear and diffractive barriers (wells). More recently, enigmas of optical and matter-wave soliton nonlinear tunneling have also been uncovered in Ref. [23]. Note that the nonlinear soliton tunneling effect is a subject of constantly renewed interest. In femtosecond nonlinear fiber optics, the most intriguing enigma of optical solitons is connected to the so-called soliton spectral tunneling effect. This effect is characterized in the spectral domain by the passage of a femtosecond soliton through a potential barrierlike spectral inhomogeneity of group velocity dispersion (GVD), including the forbidden band of positive GVD [24,25]. However, nonlinear tunneling affects other localized structures such as rogue waves and has been hardly investigated until recently.

Rogue waves for the standard NLSE have been extensively investigated [11–13]. However, the phenomenon of optical rogue waves in the femtosecond regime is significantly more complicated than the one modelled by the simple NLSE. Even in the one-dimensional case, higher-order terms, such as third-order dispersion (TOD), self-steepening (SS), and the delayed nonlinear response effect (DNRE), must be taken into account. Thus, some interesting issues arise: can optical rogue waves described by rational solutions be controlled in the femtosecond regime? What does happen when rogue waves pass through a dispersion barrier (DB) or dispersion well (DW)? To answer these problems, we consider the variable-coefficient higher-order NLSE (vcHNLSE) as follows [26–31]:

$$iu_z + D_2(z)u_{tt} + R(z)|u|^2u + iD_3(z)u_{ttt} + i\alpha(z)(|u|^2u)_t + if(z)u(|u|^2)_t = i\Gamma(z)u, \quad (1)$$

where $u(z,t)$ is the complex envelope of the electrical field and z and t, respectively, represent the propagation distance and retarded time. $D_2(z)$ and $D_3(z)$ represent the group-velocity dispersion and TOD, respectively. $R(z)$ is the nonlinearity parameter, and the parameters $\alpha(z)$ and $f(z)$ are, respectively, related to the SS and DNRE. $\Gamma(z)$ denotes the amplification or absorption coefficient.

The variable-coefficient higher-order NLSE (1) has been extensively discussed as the governing equation [26–31] for femtosecond optical soliton control, which is an important development in the application of solitons after the first soliton dispersion management experiment in a fiber with hyperbolically decreasing group-velocity dispersion was realized by Dianov's group at the General Physics Institute [32]. Then controlling optical solitons in soliton communication systems and generating soliton trains were effectively realized as early as 1991 [33]. The nonlinear Schrödinger-type equation with variable coefficients has been extensively investigated [34–37]. For vcHNLSE, many solutions, such as dark solitons [26], bright solitons [27,28], combined solitons [29], soliton trains [30], and tunneling solitons [31], have been also discussed. Therefore, a study of the vcHNLSE is significant for the concept of soliton control. However, to our knowledge, the control of rogue waves for vcHNLSE, with which this paper concerns itself, has rarely been studied.

II. GENERAL TRANSFORMATION AND SOLUTIONS

The main idea of the procedure is to transform HNLSE (1) into the constant-coefficient Hirota equation [15]

$$iU_Z + \tfrac{1}{2}U_{TT} + |U|^2U - i\alpha_3U_{TTT} - i6\alpha_3|U|^2U_T = 0, \quad (2)$$

where $U \equiv U(T,Z)$ and $T \equiv T(z,t)$ and $Z \equiv Z(z)$ are two functions to be determined.

In order to connect the solutions of Eq. (1) with those of Eq. (2), we will construct the mapping transformation [34]

$$u(z,t) = A(z)U[T(z,t),Z(z)]\exp[i\phi(z,t)], \quad (3)$$

where the amplitude $A(z)$ and the phase $\phi(z,t)$ are real functions. The substitution of Eq. (3) into Eq. (1) leads to Eq. (2), but now we must have

$$A_z - \Gamma A - 3D_3A\phi_t\phi_{tt} + D_2A\phi_{tt} = 0, \quad (4)$$

$$T_z + 2D_2T_t\phi_t - 3D_3T_t\phi_t^2 + D_3\phi_{ttt} = 0, \quad (5)$$

$$\phi_z + D_2\phi_t^2 + D_3\phi_{ttt} - D_3\phi_t^3 = 0, \quad (6)$$

$$(D_2 - 3D_3\phi_t)T_{tt} - 3D_3T_t\phi_{tt} = 0, \quad T_{tt} = 0, \quad (7)$$

$$(R - \alpha\phi_t)A^2 = Z_z, \quad 2(D_2 - 3D_3\phi_t)T_t^2 = Z_z, \quad (8)$$

$$D_3T_t^3 + \alpha_3Z_z = 0, \quad (2f + 3\alpha)A^2T_t + 6\alpha_3Z_z = 0. \quad (9)$$

After our calculations, the mapping variable, effective propagation distance, amplitude, and phase of the pulse read

$$T = k\left[t + p\left(\frac{k}{\alpha_3} - 3p\right)\int_0^z D_3(s)ds\right] + t_0, \quad (10)$$

$$Z = -\frac{k^3}{\alpha_3}\int_0^z D_3(s)ds, \quad (11)$$

$$A = A_0\exp\left[\int_0^z \Gamma(s)ds\right], \quad (12)$$

$$\phi = p\left[t + p\left(\frac{k}{2\alpha_3} - 2p\right)\int_0^z D_3(s)ds\right] + \phi_0, \quad (13)$$

where the subscript 0 denotes the initial values of the corresponding parameters at $z = 0$. Note that the TOD parameter $D_3(z)$ influences the form of the phase and effective propagation distance.

Furthermore, the constraints of the system parameters are given as

$$D_3(z) : D_2(z) : R(z) : f(z) : \alpha(z) = 1 : \left(3p - \frac{k}{2\alpha_3}\right) : \frac{k^2(2p\alpha_3 - 3k)}{3\alpha_3A_0^2\exp\left[2\int_0^z\Gamma(s)ds\right]} : \frac{2k^2}{A_0^2\exp\left[2\int_0^z\Gamma(s)ds\right]} : \frac{2k^2}{3A_0^2\exp\left[2\int_0^z\Gamma(s)ds\right]}. \quad (14)$$

Thus, we have proven the following result: the substitution

$$u = A_0U\left\{k\left[t + p\left(\frac{k}{\alpha_3} - 3p\right)\int_0^z D_3(s)ds\right] + t_0, -\frac{k^3}{\alpha_3}\int_0^z D_3(s)ds\right\}\exp\left[\int_0^z\Gamma(s)ds + i\phi\right], \quad (15)$$

where ϕ satisfies Eq. (13), leads to Eq. (2) with the condition (14). The solutions of Eq. (1) can be obtained from those of Eq. (2) via the transformation (15).

The one-to-one correspondence (15) admits us to obtain abundant solutions, such as bright and dark soliton solutions, W-shaped and M-shaped soliton solutions, and so on. With the help of the mapping transformation (15), Eq. (1) can be transformed into the Hirota NLSE (2). Then, by making the reverse transformation variables and functions, we obtain the exact solutions for Eq. (1). Here, we focus on rogue wave solutions. Employing the transformation (3) and the Darboux transformation [15], one can obtain rogue wave solutions (rational solutions) for Eq. (1). The first-order ($n = 1$) and second-order ($n = 2$) rational-like solutions read

$$u_n = A_0 \left\{ (-1)^n + \frac{G_n + i(Z - Z_0)H_n}{F_n} \right\} \exp\left[\int_0^z \Gamma(s)ds + i(Z - Z_0) + i\phi \right], \tag{16}$$

where $2G_1 = H_1 = 8$ and $F_1 = 1 + 4[T + 6\alpha_3(Z - Z_0)]^2 + 4(Z - Z_0)^2$ for a one-rogue wave and

$$\begin{aligned} G_2 = &-192T^4 - 4608T^3\alpha_3(Z - Z_0) - 288[4(36\alpha_3{}^2 + 1)(Z - Z_0)^2 + 1]T^2 \\ &- 1152\alpha_3(Z - Z_0)[12(12\alpha_3{}^2 + 1)(Z - Z_0)^2 + 7]T \\ &- 192(1296\alpha_3{}^4 + 216\alpha_3{}^2 + 5)(Z - Z_0)^4 - 864(44\alpha_3{}^2 + 1)(Z - Z_0)^2 + 36, \end{aligned} \tag{17}$$

$$\begin{aligned} H_2 = &-384T^4 - 9216\alpha_3(Z - Z_0)T^3 - 192[(432\alpha_3{}^2 + 4)(Z - Z_0)^2 - 3]T^2 \\ &- 2304\alpha_3[4(36\alpha_3{}^2 + 1)(Z - Z_0)^2 + 1](Z - Z_0)T \\ &- 384(36\alpha_3{}^2 + 1)^2(Z - Z_0)^4 - 192(180\alpha_3{}^2 + 1)(Z - Z_0)^2 + 360, \end{aligned} \tag{18}$$

$$\begin{aligned} F_2 = &\,64T^6 + 2304\alpha_3(Z - Z_0)T^5 + 48[(720\alpha_3{}^2 + 4)(Z - Z_0)^2 + 1]T^4 \\ &+ 384\alpha_3(Z - Z_0)[12(60\alpha_3{}^2 + 1)(Z - Z_0)^2 - 1]T^3 \\ &+ 12[16(6480\alpha_3{}^4 + 216\alpha_3{}^2 + 1)(Z - Z_0)^4 - 24(60\alpha_3{}^2 + 1)(Z - Z_0)^2 + 9]T^2 \\ &+ 144(Z - Z_0)\alpha_3[16(36\alpha_3{}^2 + 1)^2(Z - Z_0)^4 + (8 - 864\alpha_3{}^2)(Z - Z_0)^2 + 17]T \\ &+ 64(36\alpha_3{}^2 + 1)^3(Z - Z_0)^6 - 432(624\alpha_3{}^4 - 40\alpha_3{}^2 - 1)(Z - Z_0)^4 \\ &+ 36(556\alpha_3{}^2 + 11)(Z - Z_0)^2 + 9, \end{aligned} \tag{19}$$

for a two-rogue wave, where T and Z satisfy Eq. (10), ϕ is given by Eq. (13), and Z_0 is an arbitrary constant.

III. RECURRENCE, ANNIHILATION, AND SUSTAINMENT OF ROGUE WAVES

Next we analyze the controllable mechanism of rogue waves. The crucial point lies in the relation between the effective propagation distance Z and the original propagation distance z. To demonstrate controllable rogue waves, we first consider a soliton management system similar to that of Ref. [37], i.e., the periodic distributed system [28,29],

$$D_3 = D_{30}\cos(\kappa z), \quad \Gamma = \Gamma_0, \tag{20}$$

where D_{30} and κ are related to the TOD and Γ_0 implies a constant net gain (>0) or loss (<0). Trigonometric functions are physically relevant because they provide for alternating regions of positive and negative dispersion and nonlinearity, indicated in the improved stability of the solitons [11]. On one hand, from Eq. (10) the effective propagation distance Z is a periodical function of the original propagation distance z with $Z = -\frac{D_{30}k^3}{\alpha_3\kappa}\sin(\kappa z)$, indicating that Z changes within the domain $|Z| \leqslant Z_{\max} = |\frac{D_{30}k^3}{\alpha_3\kappa}|$. On the other hand, in the framework of Eq. (2), rogue waves reach their maximum amplitude when $Z = Z_0$ and then disappear while in the framework of Eq. (1) the complete excitation of rogue waves sustains for quite a long distance. If $Z < Z_0$, the pulse in the framework of Eq. (1) does not have a sufficient propagation distance to excite rogue waves, and the restraint (even annihilation) of rogue waves occurs. When $Z > Z_0$ for the periodic distributed system, rogue waves recur periodically. Thus, one can control behaviors of rogue waves by modulating the values of the parameters $Z_{\max}$ and Z_0.

For example, if $|\frac{D_{30}k^3}{\alpha_3\kappa}| > Z_0$, the one-rogue wave is excited from the initial value $u(0,t) = U(0,t)$ at $z = -\arcsin(\frac{Z_0\alpha_3\kappa}{k^3D_{30}})/\kappa$ and recurs periodically [cf., Fig. 1(a)]. Figures 1(c) and 1(d) display the recurrence behaviors with and without gain that can resist the perturbation of 5% white noise, which is added to the initial value by numerical simulation. As shown in Fig. 1(c) for constant gain with $\Gamma_0 = 0.001$, the energy of the system is increasing. If we do not consider gain with $\Gamma_0 = 0$, the energy of the system is unchanged [cf., Fig. 1(d)]. If $|\frac{D_{30}k^3}{\alpha_3\kappa}| < Z_0$, a rogue wave is restrained and partly excited [cf., Fig. 1(b)], which looks like a snakelike bright optical soliton with very small amplitude propagating stably along the fiber on a nonzero background. Besides controlling the excitation of rogue waves, the distributed coefficients will also change the trajectories of optical pulses. From Eq. (16), it follows that the center of mass of an optical pulse is $t_c = 6\alpha_3(Z - Z_0)$, implying, in this case, that the velocity of optical pulse is $v = 6\alpha_3$ and the center of the optical pulse oscillates periodically for $\alpha_3 \neq 0$ [cf., Fig. 1].

Based on the fact that decreasing GVD in a fiber has been realized [32], as another example, we consider an exponential dispersion decreasing fiber system [26,27,30] with

$$D_3(z) = D_{30}\exp(-\sigma z), \quad \Gamma(z) = \Gamma_0, \tag{21}$$

where D_{30} and σ are the parameters related to the TOD and Γ_0 denotes the constant net gain or loss. From Eq. (10) the effective propagation distance Z is related to the original propagation distance z with $Z = -\frac{D_{30}k^3}{\alpha_3\sigma}[1 - \exp(-\sigma z)]$, implying that when $\sigma < 0$, one has $Z > z$ and $Z \to \infty$ with $z \to \infty$; rogue waves are thus excited at $z = -\ln[1 + \frac{\sigma\alpha_3 Z_0}{D_{30}k^3}]/\sigma$ and then vanish quickly. When $\sigma > 0$, one has $Z < z$ and $Z \to -\frac{D_{30}k^3}{\alpha_3\sigma}$ with $z \to \infty$. Moreover, the centers of mass of optical waves do not change when z is large enough. Therefore,

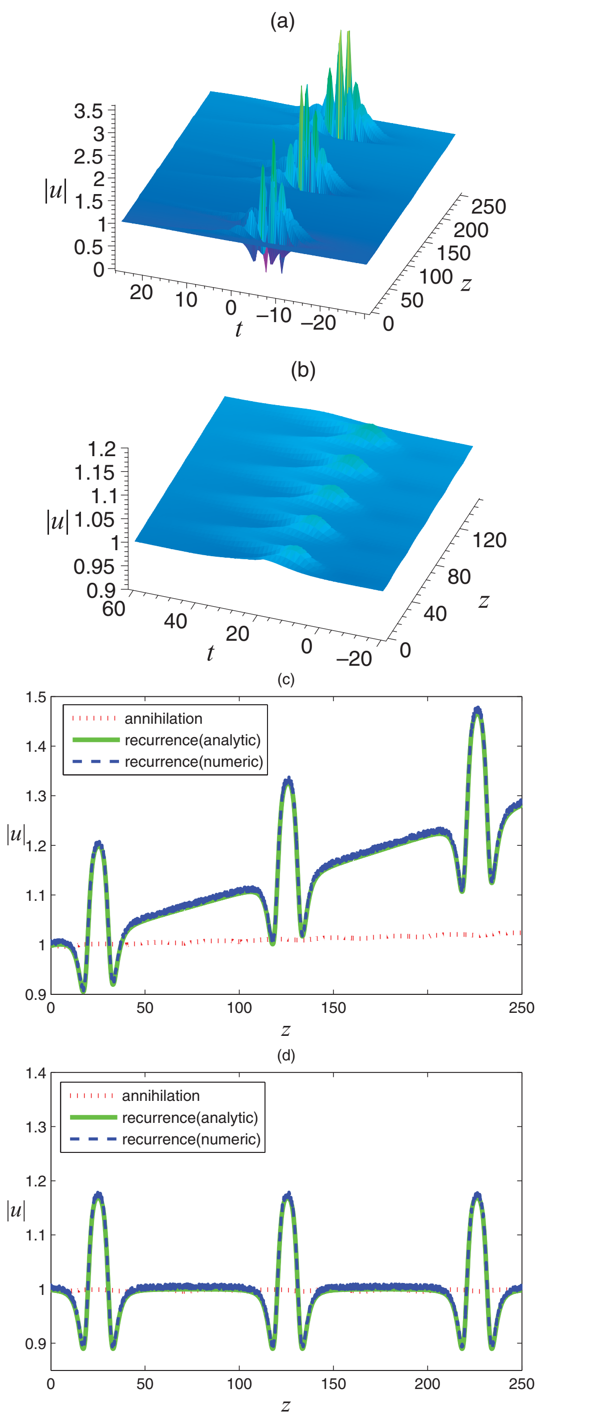

FIG. 1. (Color online) (a) Recurrence and (b) annihilation of one-rogue waves. The parameters are $A_0 = -D_{30} = 1$, $k = p = \frac{1}{2}$, $\alpha_3 = \frac{1}{5}$, $\Gamma_0 = 0.001$, $t_0 = 0$, and $Z_0 = 8$ with (a) $\kappa = \frac{1}{16}$ and (b) $\kappa = \frac{1}{5}$. (c) and (d) Sectional views of (a) and (b), respectively, at $t = -14$ with ($\Gamma_0 = 0.001$) and without ($\Gamma_0 = 0$) gain, respectively.

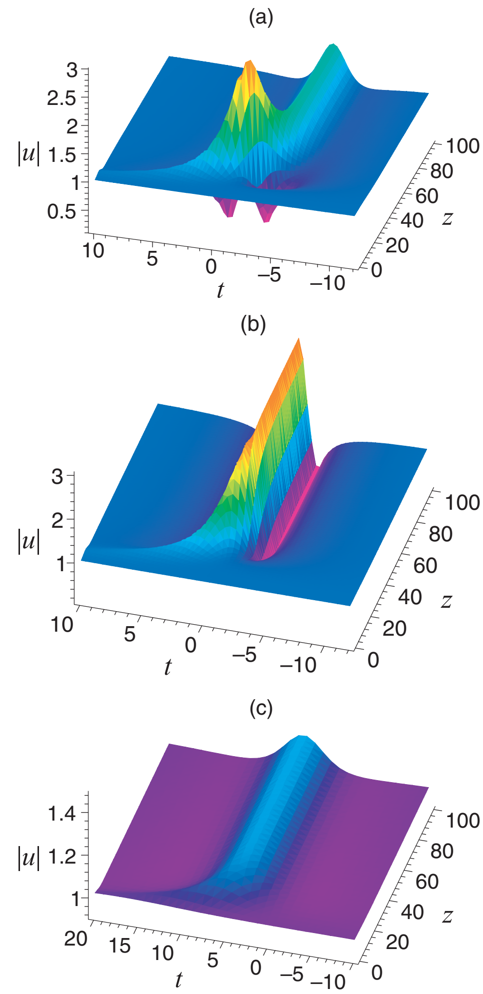

FIG. 2. (Color online) (a) Postponement, (b) sustainment, and (c) annihilation of one-rogue waves. The parameters are $k = 0.565$, $p = 1$, and $\Gamma_0 = 0.0001$ with (a) $\kappa = 0.1$, (b) $\kappa = 0.113$, and (c) $\kappa = 0.17$. Other parameters are the same as those of Fig. 1.

at first if $|\frac{D_{30}k^3}{\alpha_3\sigma}| > Z_0$, the excitations of both one-rogue wave and two-rogue waves are postponed [cf., Figs. 2(a) and 3(a)], i.e., the complete rogue waves are not excited. Secondly, if $|\frac{D_{30}k^3}{\alpha_3\sigma}| = Z_0$, the full excitations of both one-rogue wave and two-rogue waves can maintain forever [cf., Figs. 2(b) and 3(b)] as their amplitudes and widths never vary after a short propagation distance from the initial condition. Finally, if $|\frac{D_{30}k^3}{\alpha_3\sigma}| < Z_0$, the thresholds of excitation of both one-rogue wave and two-rogue waves are never reached, and their excitations, which look like bright optical solitons and separated bright soliton pairs with very small amplitudes, propagating stably along the fiber on a nonzero background, are restrained or even eliminated [cf., Figs. 2(c) and 3(c)].

In the following, we focus on rogue waves propagating through a dispersion barrier or dispersion well on an exponential background [21,22,31]:

$$D_3(z) = D_{30}\{re^{-gz} + h\text{sech}^2[a(z - z_0)]\}, \quad \Gamma(z) = \Gamma_0, \quad (22)$$

where h denotes the heights of the DB or DW, respectively. a is related to the DB or DW width, g is a decaying ($g > 0$) or increasing ($g < 0$) parameter, and z_0 represents the longitudinal coordinates indicating the locations of the DB or DW. As $\beta(z) > 0$, we assume $h > -1$, where $h > 0$ indicates a DB and $-1 < h < 0$ represents a DW. From Eq. (10) the maximum of the effective propagation distance $Z_{\max} =$

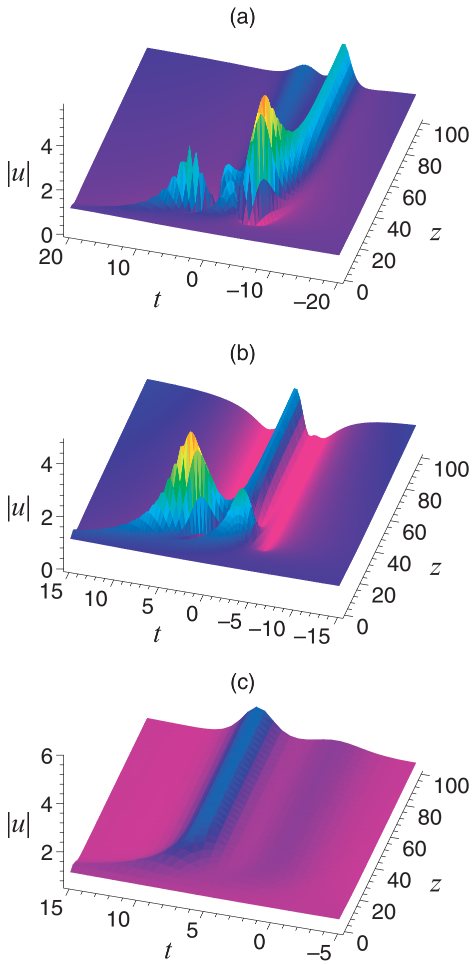

FIG. 3. (Color online) (a) Postponement, (b) sustainment, and (c) annihilation of two-rogue waves. The parameters are (a) $\kappa = 0.1$, (b) $\kappa = 0.113$, and (c) $\kappa = 0.17$. Other parameters are the same as those of Fig. 2.

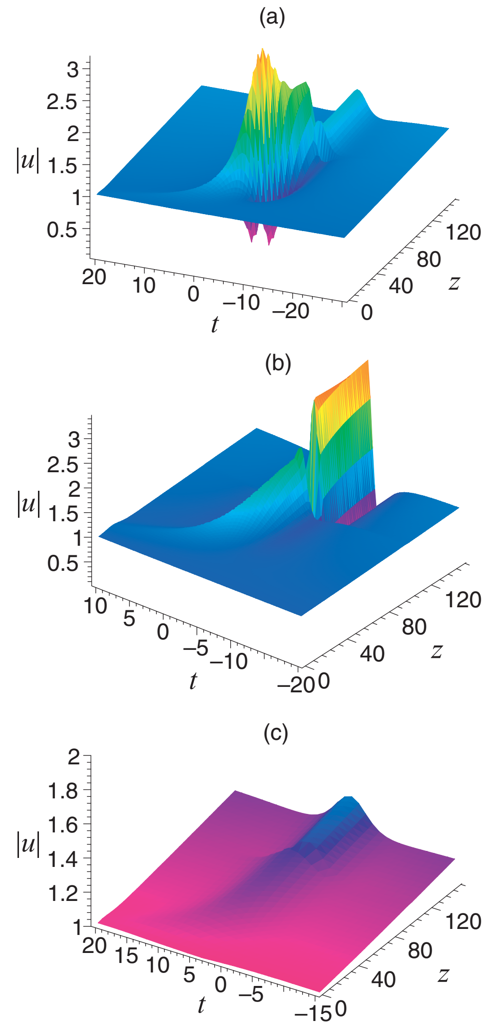

FIG. 4. (Color online) (a) Postponed, (b) sustained, and (c) annihilated one-rogue waves through the DB. The parameters are $g = 0.05$, $h = a = 1.2$, $r = p = 1$, and $z_0 = 130$ with (a) $D_{30} = -0.7$, (b) $D_{30} = -0.582$, and (c) $D_{30} = -0.4$. Other parameters are the same as those of Fig. 1.

$-\frac{k^3 D_{30}}{\alpha_3}\{\frac{h}{a}[1+\tanh(az_0)]+\frac{r}{g}\}$. Similar to discussion above, when $Z_{\max} > Z_0$, rogue waves are postponed. If $Z_{\max} = Z_0$, rogue waves can sustain, and while $Z_{\max} < Z_0$, rogue waves are restrained or even eliminated. However, the DB and DW have different effects on the postponement, sustainment, and annihilation of rogue waves. Figures 4(a) and 5(a) indicate that when the postponed rogue waves pass through the DB or DW at $z = z_0$, the amplitude diminishes or magnifies, respectively. The reverse situation exists for restrained rogue waves, whose amplitudes increase or decrease propagating through the DB or DW at $z = z_0$, respectively [cf., Figs. 4(c) and 5(c)]. Moreover, the amplitudes of maintained rogue waves invariably increase whatever they pass through, the DB or DW at $z = z_0$ [cf., Figs. 4(b) and 5(b)]. Two-rogue waves have a similar nonlinear tunneling effect. For the limit of the length, the corresponding discussions are neglected in our present paper.

At last, it is worth mentioning that a corresponding and very important problem is the stability of analytical solutions, that is, how they evolve along distance when they are disturbed from their analytically given forms. We show through a mapping transformation that a one-to-one correspondence exists between the analytical solutions of vcHNLSE and that of the constant-coefficient Hirota equation, which is stable [15]. Although this correspondence guarantees the stability of the solutions, we perform direct numerical simulations with initial white noise for Eq. (1) with initial fields coming from Eq. (16) in some cases. Five examples of such behaviors are displayed in Fig. 6, which essentially presents a numerical rerun of Figs. 2(a), 2(b), 3(a), 4(a), and 5(a). Figure 6(a) shows the comparison of analytical and numerical solutions for postponed and sustained one-rogue waves in the exponential dispersion decreasing fiber system of Eq. (21). Figure 6(b) shows the comparison of analytical and numerical solutions for postponed two-rogue waves in the exponential dispersion decreasing fiber system of Eq. (21). From them, one can find that waves are compressed along propagation distance. The comparison of analytical and numerical solutions reveals that no principal differences occur, except for some small oscillation especially in the edge of waves attached on the waves. Figures 6(c) and 6(d) display the numerical results of

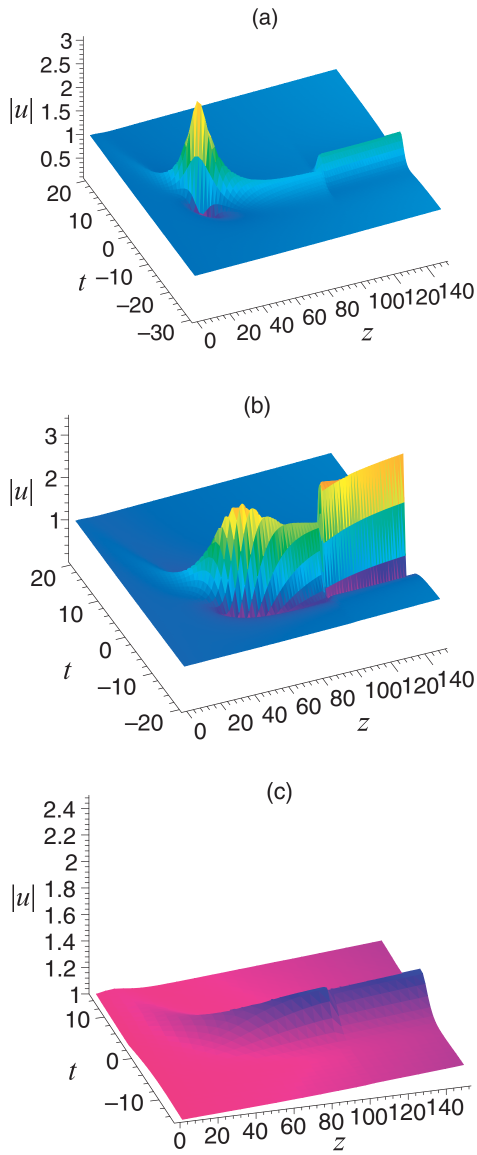

FIG. 5. (Color online) (a) Postponed, (b) sustained, and (c) annihilated one-rogue waves through the DW. The parameters are $h = -0.8$ with (a) $D_{30} = -0.8$, (b) $D_{30} = -0.686$, and (c) $D_{30} = -0.5$. Other parameters are the same as those of Fig. 4.

postponed one-rogue waves passing through the DB and DW of Eq. (22), respectively. From them, no collapses are found; instead, the stable propagation over tens of dispersion lengths are observed.

IV. CONCLUSIONS

In summary, we have constructed the relation between the vcHNLSE, describing the femtosecond pulse propagation and the constant-coefficient Hirota equation via a transformation. Based on this transformation, we analytically obtained one-rogue wave and two-rogue waves for the vcHNLSE. Under the parameter condition, we discuss the propagation behaviors of controllable rogue waves, including recurrence, annihilation, and sustainment in a periodic distributed fiber system and an

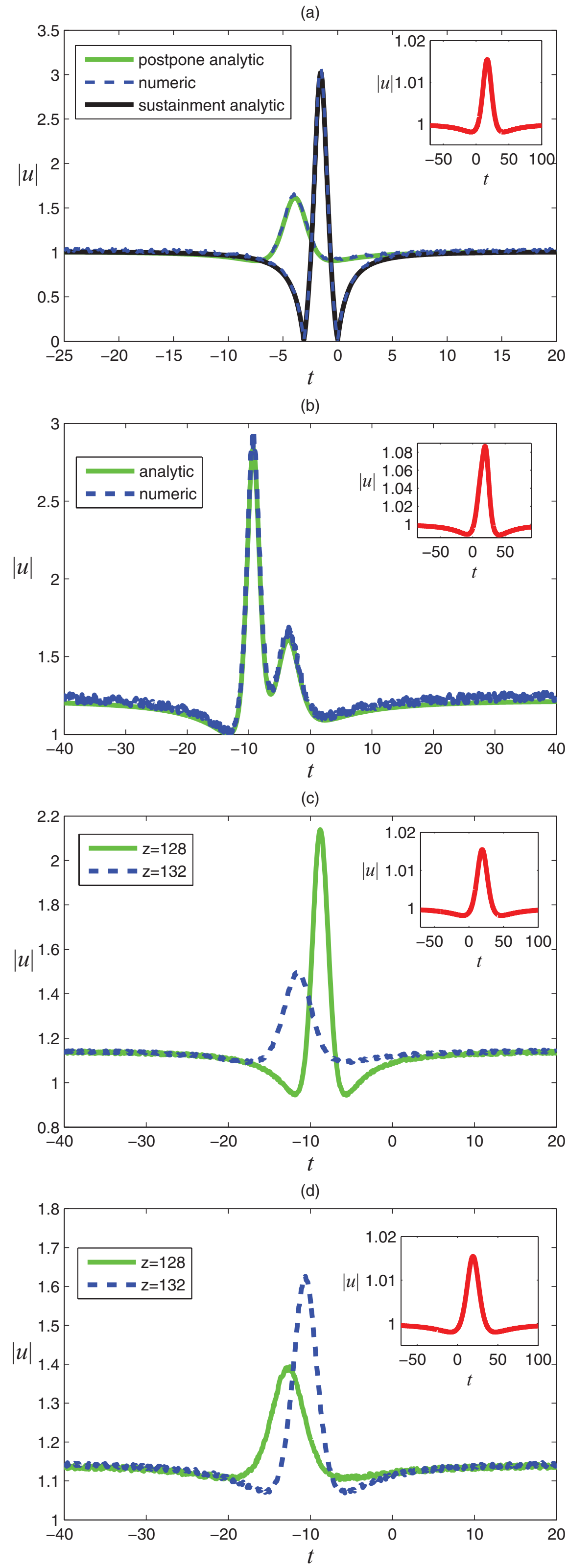

FIG. 6. (Color online) (a) Numerical simulations of (a) postponed and sustained one-rogue waves from Figs. 2(a) and 2(b) at $z = 100$ and (b) a postponed two-rogue wave from Fig. 3(a) at $z = 100$. (c) and (d) Postponed one-rogue waves passing through the DB and DW from Figs. 4(a) and 5(b), respectively. (Inset) The corresponding initial values, given by Eq. (22) with an added 5% white noise. The parameters are the same as those in the corresponding analytical plots.

exponential dispersion decreasing fiber. Also, we investigate nonlinear tunneling effects for rogue waves. These results obtained in this paper well supplement our comprehension of the rogue wave, that is, that it "appears from nowhere and disappears without a trace" [38]; rogue waves can be controlled as discussed by a similar method in this paper. Moreover, these results may have potential values for the generation and sustainment of exceptionally high-amplitude optical pulses, optical rogue waves. Of course, more practical implementations of these theoretical results might be an interesting task.

ACKNOWLEDGMENTS

The first author (C.Q. Dai) thanks Q. Tian and J. D. He for useful discussions. This work was supported by the National Natural Science Foundation of China (Grants No. 11005092, No. 10974179, No. 11072219, and No. 61178016), the Zhejiang Provincial Natural Science Foundation of China (Grant No. Y1090073), the Program for Innovative Research Team of Young Teachers (Grant No. 2009RC01), and the Scientific Research and Developed Fund (Grant No. 2009FK42) of Zhejiang Agriculture and Forestry University.

[1] W. J. Broad, *Rogue Giants at Sea* (The New York Times, New York, 2006).
[2] P. A. E. M. Janssen, J. Phys. Oceanogr. **33**, 863 (2003).
[3] N. Mori and P. A. E. M. Janssen, J. Phys. Oceanogr. **36**, 1471 (2006).
[4] D. H. Peregrine, J. Aust. Math. Soc. B **25**, 16 (1983).
[5] A. I. Dyachenko and V. E. Zakharov, JETP Lett. **81**, 255 (2005).
[6] N. Akhmediev and A. Ankiewicz, Phys. Rev. E **83**, 046603 (2011).
[7] C. Kharif, E. Pelinovsky, and A. Slyunyaev, *Rogue Waves in the Ocean* (Springer, Berlin, 2009).
[8] D. R. Solli, C. Ropers, P. Koonath, and B. Jalali, Nature (London), **450**, 1054 (2007).
[9] J. Kasparian, P. Béjot, J.-P. Wolf, and J. M. Dudley, Opt. Express **17**, 12070 (2009).
[10] N. Akhmediev and V. I. Korneev, Theor. Math. Phys. **69**, 1089 (1986).
[11] B. Kibler *et al.*, Nat. Phys. **6**, 790 (2010).
[12] M. Erkintalo, G. Genty, and J. M. Dudley, Opt. Lett. **34**, 2468 (2009).
[13] D. R. Solli, B. Jalali, and C. Ropers, Phys. Rev. Lett. **105**, 233902 (2010).
[14] A. Ankiewicz, N. Akhmediev, and J. M. Soto-Crespo, Phys. Rev. E **82**, 026602 (2010); A. Ankiewicz, N. Akhmediev, and F. Lederer, *ibid.* **83**, 056602 (2011).
[15] A. Ankiewicz, J. M. Soto-Crespo, and N. Akhmediev, Phys. Rev. E **81**, 046602 (2010).
[16] M. Erkintalo, G. Genty, and J. M. Dudley, Opt. Lett. **34**, 2468 (2009).
[17] V. N. Serkin and T. L. Belyaeva, JETP Lett. **74**, 573 (2001).
[18] A. C. Newell, J. Math. Phys. (Melville, NY, US) **19**, 1126 (1978).
[19] G. Y. Yang, R. Y. Hao, L. Li, Z. H. Li, and G. S. Zhou, Opt. Commun. **260**, 282 (2006).
[20] J. F. Wang, L. Li, and S. T. Jia, J. Opt. Soc. Am. B **25**, 1254 (2008).
[21] C. Q. Dai, Y. Y. Wang, and J. F. Zhang, Opt. Express **18**, 17548 (2010); C. Q. Dai, R. P. Chen, and J. F. Zhang, Chaos, Solitons Fractals **44**, 862 (2011).
[22] W. P. Zhong and M. R. Belic, Phys. Rev. E **81**, 056604 (2010).
[23] T. L. Belyaeva, V. N. Serkin, C. Hernandez-Tenorio, and F. Garcia-Santibanez, J. Mod. Opt. **57**, 1087 (2010).
[24] V. N. Serkin, V. A. Vysloukh, and J. R. Taylor, Electron. Lett. **29**, 12 (1993).
[25] E. N. Tsoy and C. M. de Sterke, Phys. Rev. A **76**, 043804 (2007).
[26] R. C. Yang, R. Y. Hao, L. Li, Z. H. Li, and G. S. Zhou, Opt. Commun. **242**, 285 (2004).
[27] R. Y. Hao, L. Li, Z. H. Li, and G. S. Zhou, Phys. Rev. E **70**, 066603 (2004).
[28] J. F. Zhang, Q. Yang, and C. Q. Dai, Opt. Commun. **248**, 257 (2005).
[29] R. C. Yang, L. Li, R. Y. Hao, Z. H. Li, and G. S. Zhou, Phys. Rev. E **71**, 036616 (2005).
[30] J. F. Wang, L. Li, Z. H. Li, G. S. Zhou, D. Mihalache, and B. A. Malomed, Opt. Commun. **263**, 328 (2006).
[31] K. Porsezian, A. Hasegawa, V. N. Serkin, T. L. Belyaeva, and R. Ganapathy, Phys. Lett. A **361**, 504 (2007).
[32] V. A. Bogatyrev *et al.*, J. Lightwave Technol. **9**, 561 (1991).
[33] P. V. Mamyshev, S. V. Cherinkov, and M. Dianov, IEEE J. Quantum Electron. **7**, 2347 (1991).
[34] C. Q. Dai, Y. Y. Wang, and J. F. Zhang, Opt. Lett. **35**, 1437 (2010).
[35] W. J. Liu, B. Tian, T. Xu, K. Sun, and Y. Jiang, Ann. Phys. (Amsterdam, Neth.) **325**, 1633 (2010).
[36] W. P. Zhong, M. R. Belic, Y. Q. Lu, and T. W. Huang, Phys. Rev. E **81**, 016605 (2010); N. Z. Petrovic, M. R. Belic, and W. P. Zhong, *ibid.* **83**, 026604 (2011).
[37] V. N. Serkin and A. Hasegawa, Phys. Rev. Lett. **85**, 4502 (2000); IEEE J. Sel. Top. Quant. **8**, 418 (2002).
[38] N. Akhmediev, A. Ankiewicz, and M. Taki, Phys. Lett. A **373**, 675 (2009).